Brain, Behavior, and Immunity 119 (2024) 978–988

Contents lists available at ScienceDirect

Brain Behavior and Immunity

journal homepage: www.elsevier.com/locate/ybrbi

Full-length Article

Concurrent inflammation-related brain reorganization in multiple sclerosis and depression

Lara S. Molina Galindo [a,1], Gabriel Gonzalez-Escamilla [a,1], Vinzenz Fleischer [a], Dominik Grotegerd [b], Susanne Meinert [b], Dumitru Ciolac [a], Maren Person [a], Frederike Stein [c], Katharina Brosch [c], Igor Nenadić [c], Nina Alexander [c], Tilo Kircher [c], Tim Hahn [b], Yaroslav Winter [a], Ahmed E. Othman [d], Stefan Bittner [a], Frauke Zipp [a], Udo Dannlowski [b,1], Sergiu Groppa [a,1,*]

[a] Department of Neurology, Focus Program Translational Neuroscience (FTN), Rhine-Main Neuroscience Network (rmn^2), University Medical Center of the Johannes Gutenberg University Mainz, Langenbeckstrasse 1, 55131 Mainz, Germany
[b] Institute for Translational Psychiatry, University of Münster, Münster, Germany
[c] Klinik für Psychiatrie und Psychotherapie, Philipps-Universität Marburg, Marburg, Germany
[d] Department of Neuroradiology, Rhine-Main Neuroscience Network (rmn^2), University Medical Center of the Johannes Gutenberg University Mainz, Mainz, Germany

ARTICLE INFO

Keywords:
Multiple sclerosis
Major depressive disorder
Cortical morphometric covariance
Network reorganization
Gray-to-white matter junction
Cortical morphometry

ABSTRACT

Background: Neuroinflammation affects brain tissue integrity in multiple sclerosis (MS) and may have a role in major depressive disorder (MDD). Whether advanced magnetic resonance imaging characteristics of the gray-to-white matter border serve as proxy of neuroinflammatory activity in MDD and MS remain unknown.
Methods: We included 684 participants (132 MDD patients with recurrent depressive episodes (RDE), 70 MDD patients with a single depressive episode (SDE), 222 MS patients without depressive symptoms (nMS), 58 MS patients with depressive symptoms (dMS), and 202 healthy controls (HC)). 3 T-T1w MRI-derived gray-to-white matter contrast (GWc) was used to reconstruct and characterize connectivity alterations of GWc-covariance networks by means of modularity, clustering coefficient, and degree. A cross-validated support vector machine was used to test the ability of GWc to stratify groups according to their depression symptoms, measured with BDI, at the single-subject level in MS and MDD independently.
Findings: MS and MDD patients showed increased modularity (ANOVA partial-$\eta^2 = 0.3$) and clustering (partial-$\eta^2 = 0.1$) compared to HC. In the subgroups, a linear trend analysis attested a gradient of modularity increases in the form: HC, dMS, nMS, SDE, and RDE (ANOVA partial-$\eta^2 = 0.28$, $p < 0.001$) while this trend was less evident for clustering coefficient. Reduced morphological integrity (GWc) was seen in patients with increased depressive symptoms (partial-$\eta^2 = 0.42$, $P < 0.001$) and was associated with depression scores across patient groups ($r = -0.2$, $P < 0.001$). Depressive symptoms in MS were robustly classified (88 %).
Conclusions: Similar structural network alterations in MDD and MS exist, suggesting possible common inflammatory events like demyelination, neuroinflammation that are caught by GWc analyses. These alterations may vary depending on the severity of symptoms and in the case of MS may elucidate the occurrence of comorbid depression.

1. Introduction

Multiple sclerosis (MS) is the most frequently occurring neuroinflammatory disease, accompanied by demyelination and axonal and neuronal damage (Visser-Vandewalle et al., 2022; Isensee et al., 2021). In patients with MS, comorbidities, particularly psychiatric symptoms such as depression, anxiety, and fatigue often co-occur and significantly contribute to functional impairment (Widge et al., 2019). Being depression the most prevalent psychiatric comorbidity in MS (Boeschoten et al., 2017; Widge, 2023), it relates to lower quality-of-life,

* Corresponding author.
E-mail address: segroppa@uni-mainz.de (S. Groppa).
[1] Authors contributed equally to this work.

https://doi.org/10.1016/j.bbi.2024.05.015
Received 20 December 2023; Received in revised form 2 May 2024; Accepted 12 May 2024
Available online 17 May 2024

cognitive dysfunction and disability worsening, consequently leading to an increased MS-related disease burden (Little and Brown, 2012). Depression traits in MS do not clinically differ from major depressive disorder (MDD) (Anderson et al., 2021), namely negative mood and reduced interest or pleasure of daily activities, which can be accompanied by severe somatic or vegetative symptoms (Ng et al., 2023). Recently, high involvement of the neuroimmune system in MDD has been shown (Isensee et al., 2019; Tinkhauser et al., 2018), which may relate to abnormal innate and adaptive chronic inflammatory reactions (Moraud et al., 2018). Deeper understanding of the role of the immune system for psychiatric symptoms and disorders has a vast conceptual value for the development of new immunomodulatory remedies as therapeutic interventions (Herz et al., 2018; Neumann et al., 2021). Recent work suggests that clinical features and microstructural alterations in both MS and MDD could parallel mesoscale gray matter (GM) and white matter (WM) abnormalities (Herz et al., 2022; Steffen et al., 2023). Therefore, the analysis of morphometric brain networks architecture is important for characterizing neuropathological processes in vivo (Isensee et al., 2021). In early disease stages of MS, as network reorganization occurs, even before common morphometric MRI measures can detect tissue degeneration (Isensee et al., 2021), increases in regional and modular connectivity are suggested as potential compensatory mechanisms to maintain clinical function. Afterwards, the progressive tissue damage in later disease stages leads to a network collapse in MS (Fleischer et al., 2019; Schoonheim et al., 2015). In MDD, network reorganization is detected on a regional level, particularly affecting regions involved in mood and emotion regulation (Maere et al., 2005) within the fronto-temporal circuits (Lofredi et al., 2019).

Regarding structural changes, in MS, cortical thinning is consistently found in frontal, temporal, and parietal regions (Steenwijk et al., 2016). Moreover, fronto-temporal regions show increased cortical thinning in MS patients with depressive symptoms as compared to non-depressive patients (Pravata et al., 2017). Thus, it is conceivable that maladaptive structural network reorganization involving fronto-temporal regions may contribute to the increased susceptibility to depression in MS patients (Bame et al., 2021). In MDD, many studies evidenced cortical thickening involving mostly frontal and temporal regions (Maere et al., 2005; Khawaldeh et al., 2022), while the Enhancing NeuroImaging Genetics through Meta-Analysis (ENIGMA) group has reported thinning within the same set or neighboring regions (Jacobsen et al., 2014; Brittain and Brown, 2014). However, different studies have yield small effect sizes when comparing MDD and healthy subjects (Lofredi et al., 2019; Holtzheimer et al., 2012), suggesting that brain structural effects of MDD are smaller than in MS. One possibility is that conventional measurements of brain morphometry may not fully capture the underlying neurobiological processes. Alternatively, the contrasting observations may result from different local disease-specific effects such as neuroinflammation (Kohler et al., 2017), which cannot be fully disentangled using standard morphometric parameters like cortical thickness. Early research using postmortem data and more recently using in vivo specialized brain imaging has suggested that cortical myelin, particularly in the frontal cortex, is compromised in MDD patients and that structural and molecular abnormalities of myelin integrity or myelin supporting cells is related to the clinical presentation (Sacchet and Gotlib, 2017; Sokolov, 2007; Tham et al., 2011). However a specific link between this findings and network alterations in MDD is missing. In this line, despite recent reports highlighting the involvement of neuroinflammation in the trajectory of depression (Isensee et al., 2019; Tinkhauser et al., 2018), a head-to-head comparison between MDD and primary neuroinflammatory diseases, such as MS, is missing. This is necessary in order to unveil the underlying neurobiological mechanisms of the observed morphometric changes. Recent reports on postmortem data suggest that apparent changes in cortical thickness are affected by myelin alterations in the border between GM and WM (Natu et al., 2019). Accordingly, whereas cortical thickness has been consistently used in MS research as a measurement of neurodegeneration (Isensee et al., 2021), the gray-to-white matter contrast (GWc), proposed as proxy measurement of myelin related alterations (Vidal-Pineiro et al., 2016; Kramer et al., 2015) may provide new opportunities for non-invasively investigating neuroinflammation. In MS patients (Isensee et al., 2021) and in animal models (Haider et al., 2014) demyelination is known to be immune-mediated. Recently, we evidenced GM-network reorganization already in the earliest disease stages of MS (Fleischer et al., 2017) and proposed that GWc can better delineate inflammatory damage from GM vulnerability in MS patients (Gonzalez-Escamilla et al., 2020). Under this premise, in this study, we aimed to quantify the impact of comorbid depression in MS on cortical network architecture in comparison to MDD. We now go one step further to analyze morphometric covariance networks derived from GWc and hypothesized that this imaging morphometric measurement may mirror similarities of brain pathology linking depression and neuroinflammation.

2. Subjects and methods

2.1. Participants

In total 684 participants from three different German neuroscience centers were included – Department of Neurology of the Johannes Gutenberg University Mainz, Department of Psychiatry and Psychotherapy of the Philipps-University of Marburg, and the Institute for Translational Psychiatry of the University of Münster. This included 280 MS patients from both centers, of which 222 subjects had no psychiatric comorbidity (nMS) and 58 MS patients presented depressive symptoms but no further psychiatric comorbidity (dMS). All MS patients were diagnosed with relapsing-remitting MS according to the 2010 McDonald criteria (Polman et al., 2011), were relapse-free and without steroid treatment at least sixty days prior to enrollment. Moreover, we enrolled 202 MDD patients, diagnosed according to the Structured Clinical Interview for Diagnostic and Statistical Manual of Mental Disorders IV (SCID-IV) interview (Little et al., 2016), who were divided in two groups: the first group had experienced a single depressive episode (SDE, $n = 70$) and the second group had suffered recurrent depressive episodes (RDE, $n = 132$). MDD patients did not suffer from any neurologic/psychiatric disease besides MDD according to the Structural Clinical Interview for Diagnostic (SCID-I) and Statistical Manual of Mental Disorders-IV Text Revision (DSM-IV-TR) (Wittchen et al., 1997). The control group consisted of 202 healthy participants without a history of any neurologic or psychiatric disorder. Depressed patients and healthy controls were part of the FOR2107 cohort (Münster and Marburg) (Bocci et al., 2021). All participants were matched for age and sex. The ethics committees of both centers approved the study and all patients signed the informed consent prior to participation. The FOR2107 cohort project (WP1) was approved by the Ethics Committees of the Medical Faculties, University of Marburg (AZ: 07/14) and University of Münster (AZ: 2014–422-b-S). For Mainz, the study was approved by the ethics committee of the State Medical Board of Rhineland-Palatine (approval number 837.543.11 [8085]).

2.2. Neuropsychological, clinical, and depression symptoms assessment

Depression symptom severity was evaluated with the Beck Depression Inventory (BDI) for MDD and HC (FOR2107 participants) and BDI-II for MS. Given the combination of different BDI versions and diseases, in our study a score in the range of 0–8 was considered as not having depressive symptoms, while scores greater than 8 indicated the opposite, according to proposed cutoffs (Klistorner et al., 2022). The degree of clinical disability in MS patients was determined according to the Expanded Disability Status Scale (EDSS). Patient medication regarding MS or depression symptoms were also extracted.

2.3. MRI acquisition

For all participants from the first center in Mainz, 3 T-MRI scan data were acquired on a Siemens Prisma-FIT scanner (Siemens, Germany) with a 32-channel head coil, using an anatomical 3D sagittal T1-weighted magnetization-prepared rapid acquisition with gradient echo (MPRAGE) sequence with parameters: repetition time (TR) = 1900 ms, echo time (TE) = 2.52 ms, inversion time (TI) = 900 ms, flip angle (FA) = 9°, field of view (FoV) = 256 × 256 mm^2, matrix size = 256 × 256, voxel size = 1 × 1 mm^3.

For the FOR2107 participants, two scanners have been employed. In Marburg, a 3 T MRI scanner (Tim Trio, Siemens, Erlangen, Germany) with a 12-channel head matrix Rx-coil. In Münster, a 3 T MRI scanner (Prisma, Siemens, Erlangen, Germany) with a 20-channel head matrix Rx-coil. Pulse sequence parameters were standardized across both sites to the extent permitted by each platform. Structural data was acquired using a T1-weighted 3D MPRAGE with parameters: TR = 2130 ms, TE = 2.28 ms, TI = 900 ms, FA = 8°, FoV = 256 × 256 mm^2, matrix size = 256 × 256, with an isotropic voxel size of 1 mm^3. Details of the imaging procedures and implemented quality assurance protocol have been extensively described elsewhere (Arlotti et al., 2018).

2.4. MRI preprocessing and morphometry

Individual T1-weighted data were preprocessed semi-automatically using FreeSurfer (v6.0; https://surfer.nmr.mgh.harvard.edu). Structural image processing included bias field correction, intensity normalization, lesion filling and skull stripping. Furthermore, white matter volume for both hemispheres was created, white (gray/white matter boundary) and pial (gray matter/CSF boundary) surfaces defined and corrected for topology (Fischl, 2012). To better analyze the gray-white matter boundary, intensity maps from T1-weighted images are created and then, the ratio of white to gray matter signal, i.e., gray-to-white matter contrast, is computed. Tissue intensities were measured in gray matter in a depth of 30 % of the cortical ribbon and in white matter 1 mm subjacent from the gray-white matter border (Gonzalez-Escamilla et al., 2020), and resulting values were mapped back to the cortical surface (see Fig. 1). Cortical surfaces were parceled into 68 regions (34 per hemisphere) according to the Desikan-Killiany atlas parcellation in FreeSurfer (Fischl, 2012).

2.5. Hierarchical morphometric network analyses

We computed morphometric networks derived from GWc. The network analysis was performed using a gradual approach. First, whole-cortex networks including all 68 regions were constructed for the three main groups (HC, MDD and MS). For each group, connectivity matrices were reconstructed as nodes, representing the cortical regions, and edges, representing the similarity (correlation) in between each pair of regions. The networks were reconstructed across a range of thresholds applied to the connectivity matrix (N = 64, starting at 0.3 and ending in 0.9 in 0.01 steps), allowing for statistical inference while avoiding the thresholding bias (Gonzalez-Escamilla et al., 2020). Next, we reconstructed subgroup networks and performed a global subgroup analysis, investigating differences between MDD patients with single and recurrent episodes, as well as the difference between the presence and absence of depressive symptoms in MS. As a final step of the hierarchy, according to previous work highlighting the involvement of fronto-temporal regions in depression (Maere et al., 2005; Jacobsen et al., 2014), in the further subgroup analyses 44 fronto-temporal regions (22 per hemisphere, including the cingulate cortex), defined according to FreeSurfer's lobe regional assignment (Gonzalez-Escamilla et al., 2020) (https://surfer.nmr.mgh.harvard.edu/fswiki/CorticalParcellation), were included.

2.6. Assessment of network topology

According to the relevance of network measures for evaluating neuroinflammation-related network reorganization (Fleischer et al., 2019), we analyzed modularity and clustering. Modularity measures the extent of subdivisions of the global network into groups of highly interconnected regions with sparse connections to the rest of the network (Bullmore and Sporns, 2009). The clustering coefficient evaluates the density of local connections as the number of edges between its nearest neighbours (Bullmore and Sporns, 2009).

From the reconstructed GWc networks, the regions showing differences in their degree of connectivity between groups after correction for multiple comparisons (FDR $P < 0.05$) were extracted to evidence similarity and dissimilarity among groups in regions conferring vulnerability for network reorganization.

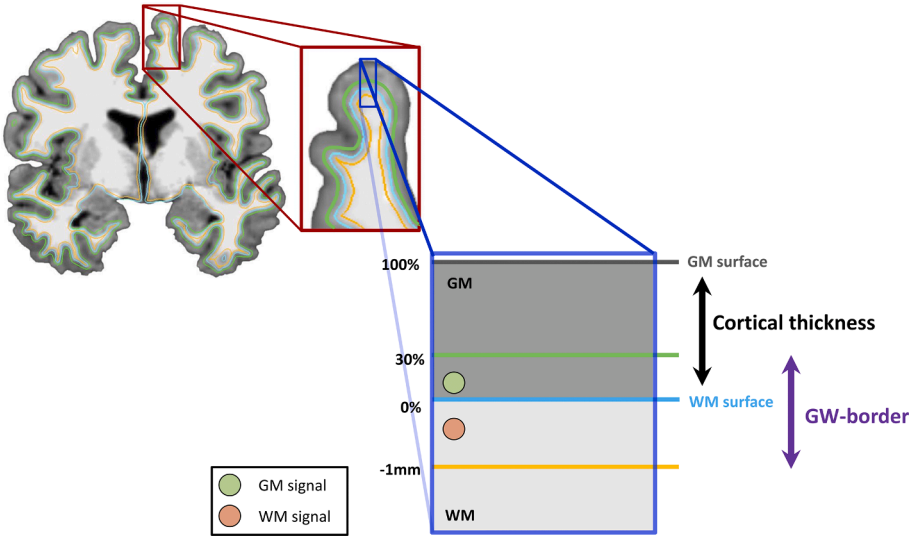

Fig. 1. Brain surface morphology metrics. Based on 3 T MRI T1-weighted images, gray-to-white matter contrast was measured based on tissue intensities, for the gray matter in a depth of 30 % from the cortical surface and in the white matter 1 mm subjacent from the gray-white matter border. The resulting intensity values were mapped to the cortical surface.

2.7. Statistical analysis

Statistical analyses were performed in Statistica™ (version 14.0; TIBCO Software) and MATLAB R2018b (Mathworks, Natick, MA, USA). One-way analysis of variance (ANOVA), χ^2-test, independent *t*-test and Mann Whitney *U* test were conducted to evaluate group differences in demographic and clinical variables, where appropriate. Network topology parameters and differences in cortical surface morphology were assessed by one-way ANOVA using group as factor (HC, SDE, RDE, nMS, and dMS) while controlling for age, sex and disease duration. Tukey–HSD post hoc analyses ($P < 0.05$) were used. A linear regression analysis was performed to test the association between global GWc and depression scores.

2.7.1. Morphometry-based classification analysis

We implemented an optimized support vector machine (SVM) classification model (Gonzalez-Escamilla et al., 2019) to estimate the discriminatory power of GWc within the MS subgroups. The SVM was trained on HC and MDD data. In this model, the classification accuracy was cross-validated via leave-one-out strategy. The trained cross-validated model was used to assess whether the morphometric parameters allow a robust classification of depressive symptoms in MS patients. Additionally, the area under the curve (AUC) from receiver operating characteristic (ROC) curves was estimated to test the sensitivity and specificity of GWc to differentiate patient subgroups from HC.

3. Results

Depressive symptoms differed significantly between subgroups (F (4, 679) = 178.41, $P < 0.001$, partial-$\eta^2 = 0.52$; Table 1). Particularly, no differences were found between dMS, SDE and RDE (post hoc $P > 0.05$), whereas these three groups had significantly higher depression scores than both nMS and HC (all $P < 0.001$). Within the MS subgroups (nMS and dMS), no differences in the level of disability as measured with EDSS or DMT (disease modifying therapy). nMS patients had a longer disease duration than dMS, whereas disease duration was longer in RDE than SDE. In MDD patients, the use of antidepressant medication was significantly more frequent in RDE than in SDE and in both MDD subgroups than in dMS. The characteristics of subjects, per subgroup including demographic and clinical information is presented in Table 1.

3.1. Group differences in whole-cortex network topology

In GWc-derived networks, we observed increased modularity (F (2, 174) = 36.4, $P < 0.001$, partial-$\eta^2 = 0.3$) and clustering (F (2, 174) = 5.2, $P = 0.006$, partial-$\eta^2 = 0.1$) across groups. Particularly, both MS and MDD patients had higher modularity and clustering in comparison to HC (Fig. 2). Higher modularity was observed in MS patients in comparison to MDD patients (Fig. 2).

3.2. Whole-cortex network subgroup analyses

The ANOVA showed that in whole-cortex GWc-derived networks both modularity (F (4, 276) = 26.12, $P < 0.001$, partial-$\eta^2 = 0.28$) and

Table 1
Characteristics of the participants.

	HC (n = 202)	nMS (n = 222)	dMS (n = 58)	SDE (n = 70)	RDE (n = 132)	Test statistic[e]	Effect size
Gender; male/female	82/120	71/151	8/50	26/43	49/84	**15.6***	**0.16**[a]
Age (in years); mean (SD)	35.7 (12.5)	34.0 (10.4)	36.4 (9.6)	36.1 (12.9)	37.9 (12.9)	1.72	0.01[b]
EDSS; median (range)	–-	1 (0–6)	1.5 (0–3.5)	–-	–-	1.15	0.01[c]
Depression score; mean (SD)	4.05 (3.88)	1.68 (2.53)	15.5 (5.97)	15.66 (11.03)	18.24 (11.29)	**178.41****	**0.52**[b,f]
Disease duration; years, mean (SD)	–-	2.3 (3.9)	1 (2.6)	7.3 (19.1)	12.4 (9.8)	**38.66****	**0.16**[b]
DMT; %	–-	75.5	64.4	–-	–-	2.31	0.1[a]
IFN		19.6	20.0				
GA		17.6	20.0				
Teriflunomide		2.0	0.0				
DMF		14.7	3.3				
Fingolimod		3.4	2.2				
Cladribine		0.0	2.2				
Natalizumab		15.2	4.4				
Alemtuzumab		0.5	0.0				
Rituximab		0.5	2.2				
Mitoxantrone		2.0	0.0				
AD; %	–-	–-	6.9	45.7	72.0	**55.70*****	**0.47**[a]
Conventional MRI-findings							
GMV; mL (SD)	707.5 (92.9)	633.7 (78.0)	621.6 (55.7)	694.5 (78.1)	700.5 (72.5)	**32.96*****	**0.16**[b]
WMV; mL (SD)	532.4 (76.4)	575.0 (82.3)	557.8 (50.4)	523.8 (59.4)	530.0 (57.0)		
	–-	6.3 (11.6)	3.4 (6.5)	–-	–-	**14.33*****	**0.08**[b]
WML; mL (SD)						1.81	0.31[d]

HC, healthy controls; nMS, non-depressed multiple sclerosis patients; dMS, multiple sclerosis patients with depressive symptoms; SDE, major depressive disorder with a single episode; RDE, major depressive disorder with recurrent episodes; EDSS, Expanded Disability Status Scale; BDI-II, Beck Depression Inventory-II; DMT, disease modifying therapy; IFN, Interferon; GA, Glatiramer acetate; DMF, Dimethyl fumarate; AD, antidepressants; GMV, gray matter volume; WMV; white matter volume; WML, white matter lesion load; mL, milliliters; SD, standard deviation.
Significant P values (<0.05) are shown in bold. *P < 0.05, **P < 0.005, ***P < 0.001.
[a] P value derived from χ^2 test, effect size is presented as phi.
[b] P value derived from one-way ANOVA, effect size is presented as patial- Eta squared (η^2).
[c] P value derived from Mann Whitney *U* test, effect size is presented as Cohen's U1.
[d] P value derived from independent *t*-test, effect size is presented as Cohens's d.
[e] χ^2/*F*-value/*Z*-value, where appropriate.
[f] Separate ANOVAS were additionally modelled for participants with BDI (HC, SDE and RDE) and BDI-II (nMS and dMS) scores. ANOVA for HC, SDE and RDE F (401,2) = 131.9, P **< 0.001,** patial-$\eta^2 = 0.4$; ANOVA for nMS and dMS F(278,1) = 711.6, P **< 0.001**, patial-$\eta^2 = 0.72$.

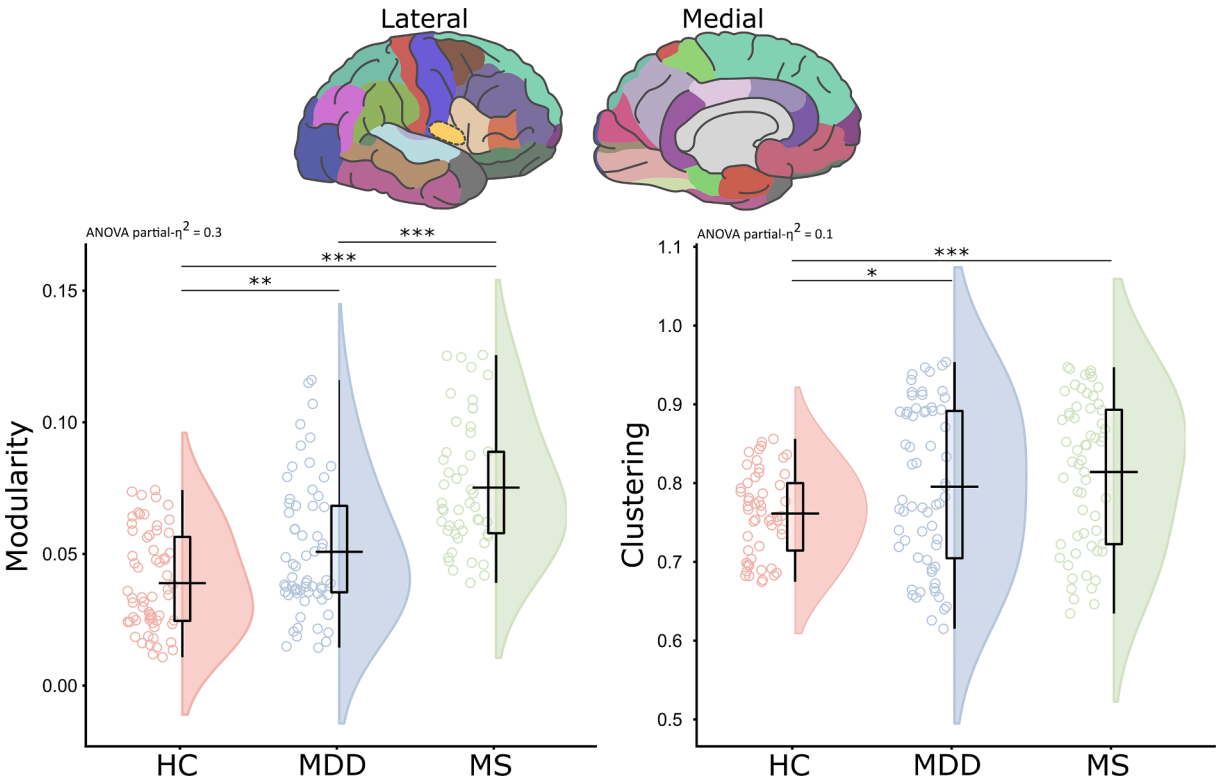

Fig. 2. Differences in modularity and clustering coefficient across groups. Network parameters of morphometric covariance networks derived from gray-to-white matter contrast in the three main groups: healthy controls (HC), multiple sclerosis (MS) and major depressive disorder (MDD). For each network parameter an ANOVA was used, followed by Tukey-HSD post-hoc analysis to evaluate pair-wise differences between the groups ($P < 0.05$). *$P < 0.05$, **$P < 0.005$, ***$P < 0.001$.

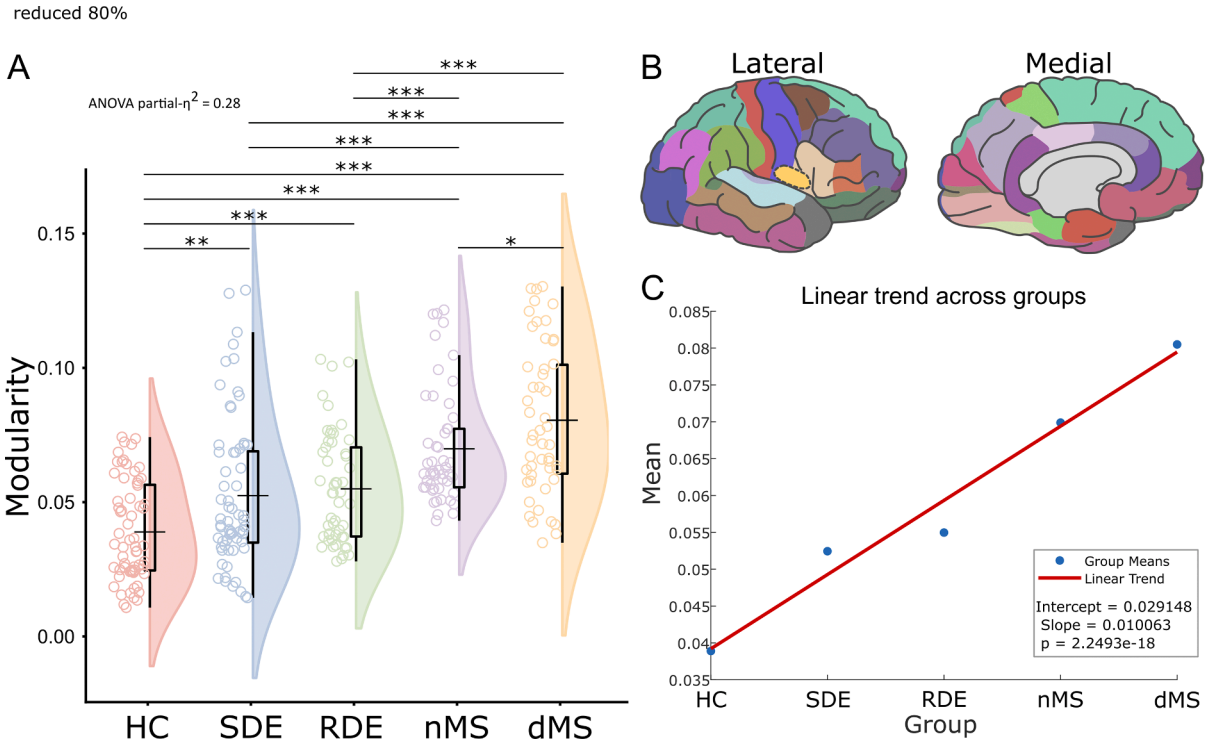

Fig. 3. Subgroup differences in whole-cortex network topology. A) Increased modularity as derived from morphometric covariance networks based on gray-to-white matter contrast in major depressive disorder with single (SDE) and recurrent depressive episodes (RDE), multiple sclerosis patients without depression symptoms (nMS), and multiple sclerosis with depressive symptoms (dMS) compared to healthy controls (HC). Post-hoc analyses for differences between groups were calculated with Tukey-HSD ($P < 0.05$). *$P < 0.05$, **$P < 0.005$, ***$P < 0.001$. B) Depiction of the cortical regions included in the reconstruction of the GW contrast networks, according to the cortical segmentation form Freesurfer. C) Linear trend analysis evidencing a statistically significant gradient of modularity increases across groups.

clustering (F (4, 276) = 3.36, P = 0.01, partial-η^2 = 0.04) differed significantly among the subgroups. Specifically, for modularity a gradient of increase was observed in the direction HC < SDE < RDE < nMS < dMS (all P < 0.005; Fig. 3). MS subgroups differed from the depression subgroups (all P < 0.001), and increased modularity was observed in dMS when compared to nMS (P = 0.036). For clustering, patient subgroups showed a significant increase in comparison to HC (all P < 0.05). A similar pattern of increased gradient emerged within the subgroups, but only differences between SDE and nMS were significant (P < 0.05).

3.3. Fronto-temporal network reorganization in MS and MDD

The network analysis including the fronto-temporal regions (Fig. 4) evidenced a significant increase in modularity (F (4, 271) = 15.8, P < 0.001, partial-η^2 = 0.19) but not for clustering (F (4, 271) = 1.77, P = 0.065 partial-η^2 = 0.023). The pattern of differences here showed main differences for all groups to HC (all P < 0.001). Increased modularity was observed among nMS, dMS and RDE, as well as between dMS and SDE (all P < 0.05; Fig. 4).

3.4. Regional similarities on network vulnerability

Our analyses evidenced that the number of vulnerable regions, i.e. with significant influence on network reorganization, was greater in RDE and both MS subgroups in comparison to SDE (see Table 2). Across subgroups a predominance of fronto-temporal regions (including the cingulate) was evident. Interestingly, in all patient subgroups the entorhinal cortex was the area with the highest degree, and the only area identified as a network hub (i.e., region with degree above 2 standard deviations than the mean network degree). Accordingly, the entorhinal cortex showed network topology (degree) differences across SDE, RDE and dMS subgroups when compared to HC (Table 2). A robust linear regression analysis between the structural integrity of the entorhinal cortex and BDI-scores, revealed that the severity of depressive symptoms was associated with increased GWc abnormalities across all patients (r = 0.39, P < 0.001) but not in HC (r = -0.126, P > 0.05).

3.5. Cortical morphometry differentially correspond to depressive symptomatology

When comparing the cortical morphometry among the three main groups (HC, MDD, and MS) (Fig. 5), group differences across all cortical regions showed a similar pattern of GWc (F (2, 681) = 247.2, P < 0.001, partial-η^2 = 0.42). More specifically, GWc decreased in MS compared to MDD and HC (all P < 0.001), without noticeable differences between MDD and HC (P > 0.05).

When subdividing the MDD and MS groups, again reduced GWc was observed (F (4, 679) = 125.04, P < 0.001, partial-η^2 = 0.42), but contrary to the network analyses no clear differences among all subgroups were attested. For GWc, significant differences appeared only between MS subgroups and HC as well as between MS subgroups and MDD subgroups (all P < 0.001), whereas no differences were seen between SDE and RDE when compared to HC, nor between SDE and RDE or nMS

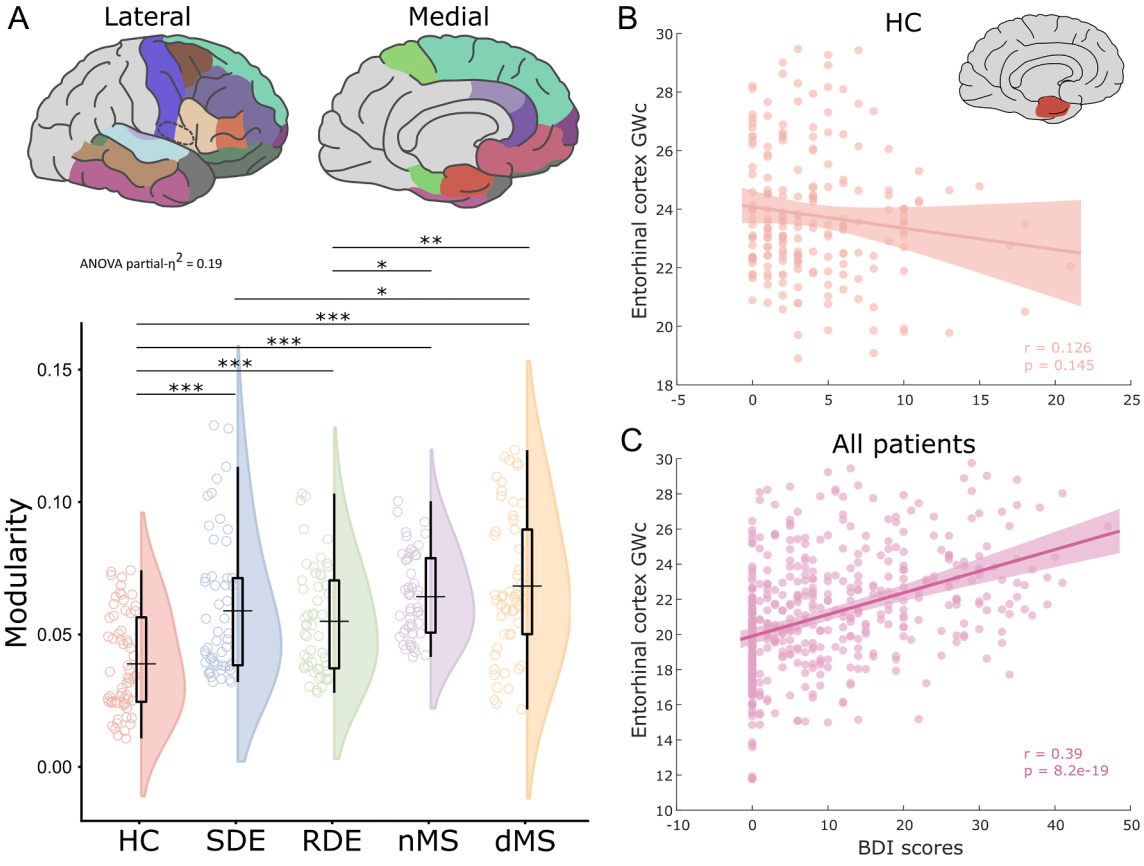

Fig. 4. Subgroup differences in fronto-temporal network topology. A) Forty-four fronto-temporal regions were included as defined by FreeSurfer lobe segmentation (see methods). The ANOVA evidenced increased modularity as derived from morphometric covariance networks based on gray-to-white matter contrast in major depressive disorder with a single (SDE) and recurrent depressive episodes (RDE), multiple sclerosis patients without depressive symptoms (nMS), and multiple sclerosis patients with depressive symptoms (dMS) in comparison to healthy controls (HC). Post-hoc analyses for differences between groups were calculated with Tukey-HSD (P < 0.05). *P < 0.05, **P < 0.005, ***P < 0.001. We further assessed the association between depression symptoms severity, assessed via BDI, and the morphological integrity of the entorhinal cortex (marked in red in the upper right gray small brain), which resulted non-significant in HC (B) but significant in the included patients (C). (For interpretation of the references to colour in this figure legend, the reader is referred to the web version of this article.)

Table 2
Regional subgroup differences in network degree as indicator of higher vulnerability.

SDE		RDE		nMS		dMS	
regions (n = 3)	P*	regions (n = 11)	P*	regions (n = 11)	P*	regions (n = 7)	P*
Left hemisphere							
isthmus cingulate	0.01	postcentral	<0.001	middle temporal	<0.001	parahippocampal	<0.001
bankssts	0.03	posterior cingulate	0.01	caudal middle frontal	0.01	lingual	0.02
entorhinal	0.045	pars opercularis	0.03	pars orbitalis	0.02	pars orbitalis	0.04
		lingual	0.03	inferior temporal	0.04	isthmus cingulate	0.04
		pericalcarine	0.04	pericalcarine	0.04		
		temporal pole	0.045				
Right hemisphere							
		entorhinal	<0.001	paracentral	0.03	entorhinal	0.01
		postcentral	<0.001	caudal anterior cingulate	0.04	bankssts	0.03
		pericalcarine	<0.001	transverse temporal	0.04	inferior temporal	0.03
		posterior cingulate	0.03	fusiform	0.04		
		parahippocampal	0.03	caudal middle frontal	0.045		
				middle temporal	0.045		

bankssts = banks of superior temporal sulcus; SDE = major depressive disorder with a single depressive episode; RDE = major depressive disorder with recurrent depressive episodes; nMS = multiple sclerosis patients without depressive symptoms; dMS = multiple sclerosis patients with depressive symptoms.
* P-values are shown after FDR correction with a threshold of 95% confidence.

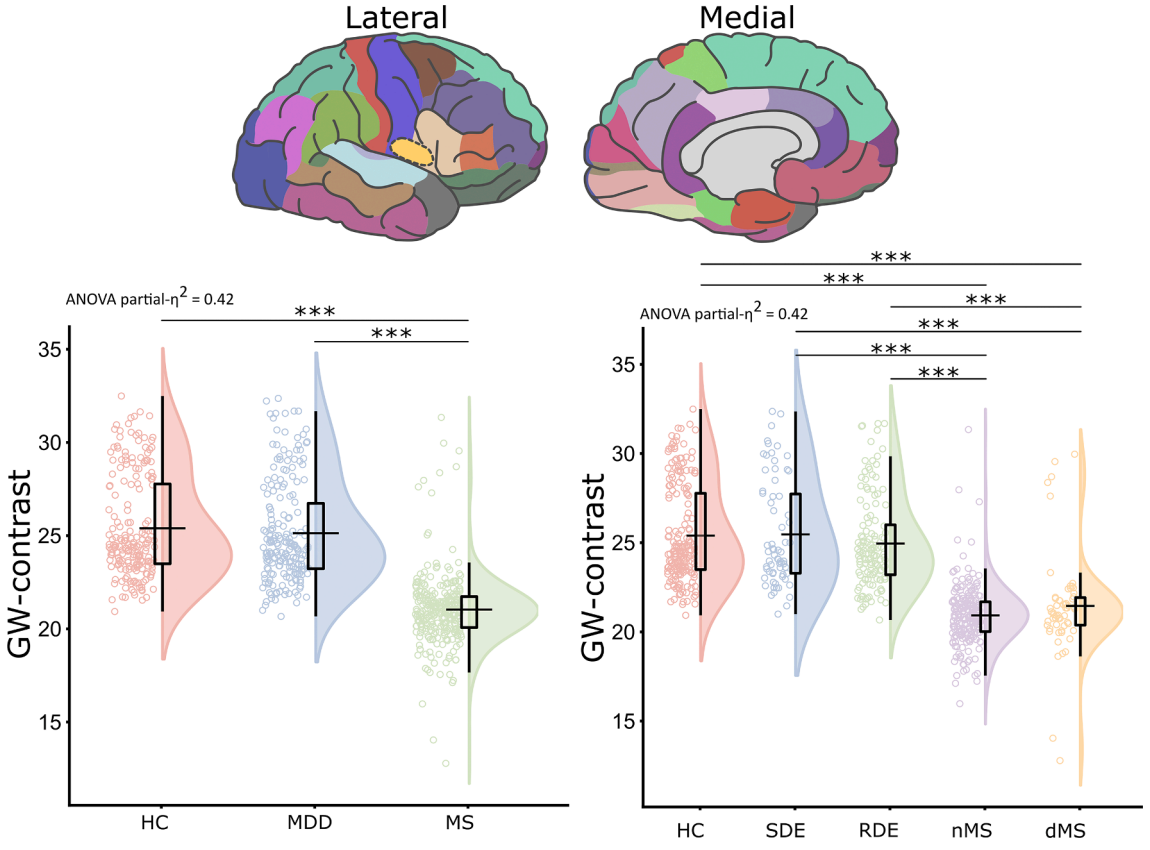

Fig. 5. Morphometric differences between groups. For the main groups and subgroups, reductions in gray-to-white matter contrast (GW-contrast) were attested. Post-hoc pair-wise differences were calculated with Tukey-HSD. Only significant results ($p < 0.05$) are shown. Healthy controls (HC), major depressive disorder patients (MDD) with a single episode (SDE), MDD with recurrent episodes (RDE), and multiple sclerosis (MS) patients with no symptoms of depression (nMS), and MS patients with depressive symptoms (dMS).

and dMS.

GWc in the fronto-temporal regions showed significant group differences ($F(4, 679) = 117.22$, $P < 0.001$, partial-$\eta^2 = 0.41$). Post-hoc analysis revealed decreased GWc in nMS and dMS to all groups (all $P < 0.05$), whereas no differences between HC and SDE or RDE were observed. Thus, in comparison to the network analyses, pure morphometric approaches may not provide enough sensitivity to follow the clinical presentation of MDD.

In order to further shed light onto the value of GWc on depression symptoms, we first trained a SVM to distinguish between HC and depression patients reaching a 75 % leave-one-out cross-validated accuracy of. The validation accuracy reached 84 % for classifying nMS patients and 88 % for classifying dMS (Fig. 6). We further tested, through ROC analysis, the discriminative value of GWc for

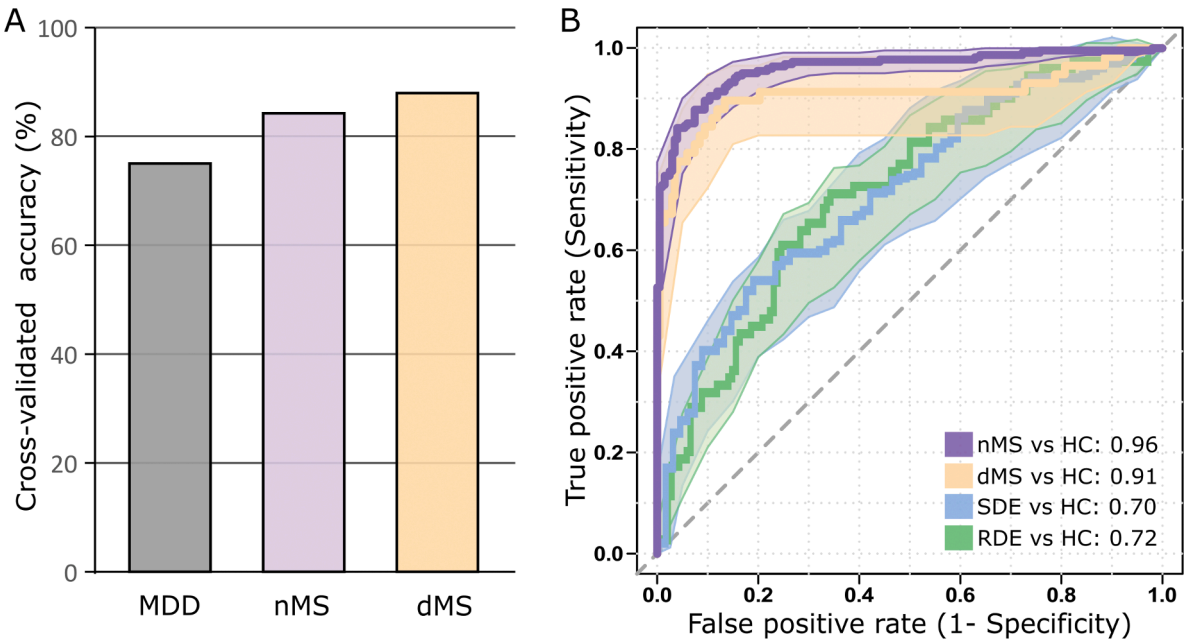

Fig. 6. Differentiation of multiple sclerosis, major depressive disorder and healthy controls. (A) Cross-validated accuracy (%) of the support vector machine classification of depression symptoms among MS patients; the higher accuracy was attested for multiple sclerosis patients with depressive symptoms (dMS; 88%) followed by non-depressed multiple sclerosis (nMS; 84%). (**B**) The receiver operating characteristic (ROC) curves with their respective area under the curve (AUC) depict the performance of whole-cortex gray-to-white matter contrast (GW-contrast) in differentiating nMS and dMS against HC, as well as for major depressive disorder patients with a single depressive episode (SDE) and major depressive disorder patients with recurrent depressive episodes (RDE) against HC.

distinguishing between patient subgroups and HC. GWc discriminated at best between HC and nMS (AUC = 0.96), followed by dMS (AUC = 0.91). Lower performance was achieved between HC and SDE (AUC = 0.7) and RDE (AUC = 0.72).

4. Discussion

By evaluating cortical morphometric covariance networks of MS patients with and without depressive symptoms in comparison to MDD and HC, we attempted to disentangle the effects of comorbidity and disease severity on cortical network reorganization. The demonstrated similarities in network reorganization between MS and MDD indicate the involvement of neuroinflammation in patients with MDD and may underlie the increased vulnerability of MS patients to develop depressive symptoms.

4.1. Network reorganization in MDD resembles neuroinflammation-related reorganization

In MS patients, neuroimmune-related cortical network reorganization, as reflected by increased topology metrics, is detectable very early in the disease trajectory, even before gray matter atrophy becomes manifest and is related to the clinical phenotype (Isensee et al., 2021; Müller et al., 2023). In the early stages of MS, a decomposition of the network into smaller modules is widely interpreted as an adaptive mechanism to maintain brain function despite long-range disconnection (Isensee et al., 2021; Schoonheim et al., 2015). This increase in modularity was also evidenced in our study. However, here, increased modularity closely reflected the severity in depression in both MDD subgroups and the comorbidity in MS patients, depicting a significant linear trend (gradient) of the form dMS > nMS > RDE > SDE > HC. Interestingly, the clustering coefficient increased in all groups when compared to HC, but not among them. In view of the observed modularity pattern, this may reflect an adaptive mechanism in which local connections are strengthened in response to an ongoing loss of long-range connections between subnetworks (Isensee et al., 2021; Fleischer et al., 2017), whereas the lack of alterations in clustering among subgroups strongly suggests the involvement of similar mechanisms underlying network organization. We propose that brain inflammation contributes to network reorganization in MDD and increase vulnerability to depression in MS patients. This is supported by previous reports on increased network topology in MS patients mirroring ongoing neuroinflammation (Ciolac et al., 2019) (see Groppa et al. (Isensee et al., 2021) for a recent review). Moreover, recent findings have posed a major role of neuroinflammation in MDD (Isensee et al., 2019; Tinkhauser et al., 2018). Peripheral inflammatory markers are linked to a disturbed white matter integrity underpinning the relevance of inflammation on myeloarchitecture (Vercellino et al., 2008). In MS, a direct link between neuroinflammation and depression has been recently evidenced (Gonzalez-Escamilla et al., 2022; Tinkhauser et al., 2017).

4.2. The added value of GW-contrast for assessing neuroinflammation and brain reorganization

GWc has been proposed to assess myelin-related alterations within the GW-boundary, (Vidal-Pineiro et al., 2016; Kramer et al., 2015)which in MS are known to be immune-mediated (Isensee et al., 2021). In the cuprizone animal model of inflammatory demyelination a decrease in GWc during demyelination phase has been reported (Haider et al., 2014). Histological correlates of cortical structural network alterations in a post-mortem sample of MS patients evidenced an association of integration and segregation parameters with neuronal size and axonal density (Steffen et al., 2023), therefore in MS patients GWc network-derived topology likely depicts neuroimmune-related aspects of tissue reorganization (Gonzalez-Escamilla et al., 2020).

In MDD patients, our findings of reduced GWc are supported by previous postmortem MDD and quantitative MRI studies reporting reduced myelin in the cortex and superficial white matter (Duchet et al., 2021; Ricigliano et al., 2021). Possible explanations comprise neuroinflammation −mediated effects, as elevated cytokine concentrations in blood (Elkjaer et al., 2021), cerebrospinal fluid (Assarsson et al., 2014) as well as in post-mortem brain tissue (Szklarczyk et al., 2021) exist in

depressed patients. Some of these cytokines like tumor necrosis factor (TNF)-α induce oligodendrocyte apoptosis via direct cytotoxicity (Huang et al., 2020). Defects of oligodendrocyte lineage cells lead to disturbed myelination, which may account for interindividual vulnerability to depressive symptoms (Giordano et al., 2022). Reduced oligodendrocyte density is found in post-mortem brain samples of MDD patients (Assarsson et al., 2014). Therefore, reduced myelin content, captured by GWc, is a potential proxy for the neuroinflammatoy activity in MDD and MS. Indeed, treatment with antidepressant medication has an anti-inflammatory effect by cytokine reduction (Engel et al., 2020) and can therefore shape myeloarchitecture and the GWc-signal. This is underpinned by studies of MS mouse models showing that that treatment with venlafaxine reduces demyelination in cuprizone mice while fluvoxamine mitigates inflammation and demyelination in experimental autoimmune encephalitis (Steffen et al., 2023; Parodi and Kerlero de Rosbo, 2021). In our study, use of antidepressants in the MDD subgroups might have reduced the effect on GWc signal by above mentioned mechanisms, while in the MS patients only about 7 % of the depressed participants were on antidepresants. Likewise, effects could be comparatively more severe in dMS due to absent antidepressant medication.

Altogether, GWc may be rendered a more sensitive proxy for neuroinflammation-associated myelin-related alterations, while cortical thickness remains a sensitive proxy for neurodegeneration. Both brain morphometric parameters mirroring parallel processes of tissue remodeling that can be considered complementary to each other, offering a more comprehensive assessment of gray matter pathology. Further research should address the underlying histologic processes to elucidate their neuropathological basis.

4.3. Reduced cortical integrity increases vulnerability to depressive symptoms in MS

In accordance with the network analyses, MS patients with depressive symptoms presented reduction of the GWc and more pronounced network abnormalities. In accordance, depressive symptoms in MS have been linked to cortical integrity abnormalities in the temporal (Maere et al., 2005; Chen et al., 2018) and fronto-temporal (Pravata et al., 2017; Tham et al., 2011) regions. Two possible hypothesis may serve to explain the current results, first depressive symptomatology may have a cumulative effect on the preexisting neural damage in MS. Alternatively, neural damage related to neuroinflammation and demyelination in MS may drive depression symptoms. Noteworthy, across all patient subgroups, the entorhinal cortex was the only area that exhibited hub properties and, thereby posed the highest vulnerability to the network. Due to its core position as component of the upstream hippocampal circuitry, the entorhinal cortex provides excitatory inputs to the hippocampus via the perforant pathway and the entorhinal layer IV receives one of the major efferent projections from the hippocampus. Additionally we found an association between structural damage in the entorhinal cortex (abnormal GWc) and increased depressive symptoms. A recent study reported an association of entorhinal integrity and increase of depressive symptoms in depressed patients with elevated peripheral inflammatory markers, which was suggested as an indicator of entorhinal cortex increased vulnerability to inflammation in MDD-patients (Sacco et al., 2016). Altogether, this suggests that a combination of network- and microstructure-mediated effects account for the increased susceptibility to developing depressive symptoms in MS and further episodes in MDD.

Overall, we evidenced that depressive symptoms are associated with alterations in the organization of morphometric networks that overlapped with neuroinflammation-related reorganization. Depressive symptoms in MS and recurrent depression episodes in MDD showed to have a cumulative effect on aberrant cortical connectivity but similar in topology. Altogether, we show that network reorganization related to depression is overlapping with neuroinflammatory patterns. GW-contrast analyses serve as a valuable complementary morphometric parameter that allows detection of subtle alterations related to clinical manifestations.

4.4. Limitations of study

There are limitations of our study. A first limitation is that different versions of the BDI depression scale were used (BDI-I and BDI-II). However, the revised version (BDI-II) only included small adaptation of the wording to better fit the DSM-IV criteria for depression and in a comprehensive review a high correlation between both BDI versions was found (Wang and Gorenstein, 2013). Moreover, we opted to use a cut-off of 8 points for the BDI scales, which is within the widely-used ranges (Wang and Gorenstein, 2013) although being lower than other suggested cut-offs determined for MS (Sacco et al., 2016), and despite non comparable, both BDI-I and −II are well-validated for the assessment of depressive symptoms in MDD and MS. (Sacco et al., 2016; Kühner et al., 2007) Nonetheless, the use of any arbitrary threshold might led to uncertain inclusion of participant in the subgroups. A plausible solution to combine test would be the usage of metrics transformation methods https://www.common-metrics.org/. Unfortunately the mentioned method is still not validated and require measurement of same lengths, which are not always available in multi-centric studies. Related to this, we have based our analyses on one single depression score, but others are available, which have a different sensitivity are shown to be complementary measurements (Seemuller et al., 2023), such as the Hamilton Depression Rating Scale (HAM-D) and the Montgomery Asberg Depression Rating Scale (MADRS). Further, the two main cohorts of patients were scanner in different scanners, resulting in uneven distribution of the groups across scanners. Although correction for scanner can be included in the statistical models for HC and MDD, inclusion of this confounding factor in MS may narrow the disease effects of interest. However, the MRI acquisition parameters, particularly the TI were comparable across centers. Noteworthy, the morphometric measurements of all groups were found to fall well into the range of the other groups (GWc values [20.7–32.4]). Noteworthy, the exact link between neuroinflammation, demyelination and symptom severity remain to be fully elucidated, for this endeavor further longitudinal studies with myelin sensitive imaging are necessary and possibly substantiated with histological data are needed. Additionally, not enough information was available to evaluate possible effects of medication over the myeloarchitecture and the GWc-signal. Finally, despite using nonspecific markers of neuroinflammation, as above discussed previous post-mortem and animal reports guaranty the link between GWc and ongoing neuroinflammation.

Funding

This work was supported by the German Research Foundation (Deutsche Forschungsgemeinschaft, DFG; CRC-TR-128). The FOR2107 consortium is supported by the DFG (Grant nos. KI 588/14–1, KI 588/14–2, KR 3822/7–1, KR 3822/7–2, NE 2254/1–2, DA 1151/5–1, DA 1151/5–2, SCHW 559/14–1, GA 545/7–2, RI 908/11–2, WI 3439/3–2, NO 246/10–2, DE 1614/3–2, HA 7070/2–2, JA 1890/7–1, JA 1890/7–2, MU 1315/8–2, RE 737/20–2, KI 588/17–1).

CRediT authorship contribution statement

Lara S. Molina Galindo: Writing – original draft, Investigation, Formal analysis. **Gabriel Gonzalez-Escamilla:** Writing – review & editing, Writing – original draft, Visualization, Software, Methodology, Formal analysis, Data curation, Conceptualization. **Vinzenz Fleischer:** Writing – review & editing, Data curation. **Dominik Grotegerd:** Data curation. **Susanne Meinert:** Data curation. **Dumitru Ciolac:** Writing – review & editing, Data curation. **Maren Person:** Data curation. **Frederike Stein:** Data curation. **Katharina Brosch:** Data curation. **Igor**

Nenadić: Funding acquisition, Data curation. **Nina Alexander:** Data curation. **Tilo Kircher:** Writing – review & editing, Project administration, Funding acquisition, Data curation. **Tim Hahn:** Writing – review & editing, Funding acquisition, Data curation. **Yaroslav Winter:** Writing – review & editing. **Ahmed E. Othman:** Writing – review & editing. **Stefan Bittner:** Data curation. **Frauke Zipp:** Data curation. **Udo Dannlowski:** Writing – review & editing, Project administration, Funding acquisition. **Sergiu Groppa:** Writing – review & editing, Supervision, Funding acquisition, Conceptualization.

Declaration of competing interest

The authors declare that they have no known competing financial interests or personal relationships that could have appeared to influence the work reported in this paper.

Data availability

Data will be made available on request.

Acknowledgements

Parts of this research were conducted using the supercomputer Mogon and/or advisory services offered by Johannes Gutenberg University Mainz (hpc.uni-mainz.de), which is a member of the AHRP and the Gauss Alliance e.V. We are thankful to the participants for their time and effort. The authors thank Kathleen Claussen for proof reading the manuscript.

References

Anderson, R.W., Wilkins, K.B., Parker, J.E., et al., 2021. Lack of progression of beta dynamics after long-term subthalamic neurostimulation. Ann. Clin. Transl. Neurol. 8 (11), 2110–2120.
Arlotti, M., Marceglia, S., Foffani, G., et al., 2018. Eight-hours adaptive deep brain stimulation in patients with Parkinson disease. Neurology 90 (11), e971–e976.
Assarsson, E., Lundberg, M., Holmquist, G., et al., 2014. Homogenous 96-plex PEA immunoassay exhibiting high sensitivity, specificity, and excellent scalability. PLoS One 9 (4), e95192.
Bame, E., Tang, H., Burns, J.C., et al., 2021. Next-generation Bruton's tyrosine kinase inhibitor BIIB091 selectively and potently inhibits B cell and Fc receptor signaling and downstream functions in B cells and myeloid cells. Clin. Transl. Immunol. 10 (6), e1295.
Bocci, T., Prenassi, M., Arlotti, M., et al., 2021. Eight-hours conventional versus adaptive deep brain stimulation of the subthalamic nucleus in Parkinson's disease. npj Parkinson's Dis. 7 (1), 88.
Boeschoten, R.E., Braamse, A.M.J., Beekman, A.T.F., et al., 2017. Prevalence of depression and anxiety in Multiple Sclerosis: A systematic review and meta-analysis. J Neurol Sci. 15 (372), 331–341.
Brittain, J.S., Brown, P., 2014. Oscillations and the basal ganglia: motor control and beyond. NeuroImage 85 (Pt 2), 637–647.
Bullmore, E., Sporns, O., 2009. Complex brain networks: graph theoretical analysis of structural and functional systems. Nat Rev Neurosci. 10 (3), 186–198.
Chen, S., Zhou, Y., Chen, Y., Gu, J., 2018. fastp: an ultra-fast all-in-one FASTQ preprocessor. Bioinformatics 34 (17), i884–i890.
Ciolac, D., Luessi, F., Gonzalez-Escamilla, G., et al., 2019. Selective brain network and cellular responses upon dimethyl fumarate immunomodulation in multiple sclerosis. Front Immunol. 10, 1779.
Duchet, B., Ghezzi, F., Weerasinghe, G., et al., 2021. Average beta burst duration profiles provide a signature of dynamical changes between the ON and OFF medication states in Parkinson's disease. PLoS Comput Biol. 17 (7), e1009116.
Elkjaer, M.L., Nawrocki, A., Kacprowski, T., et al., 2021. CSF proteome in multiple sclerosis subtypes related to brain lesion transcriptomes. Sci. Rep. 11 (1), 4132.
Engel, S., Steffen, F., Uphaus, T., et al., 2020. Association of intrathecal pleocytosis and IgG synthesis with axonal damage in early MS. Neurology(r) Neuroimmunology & Neuroinflammation. 7 (3).
Fischl, B., 2012. FreeSurfer. Neuroimage. 62 (2), 774–781.
Fleischer, V., Groger, A., Koirala, N., et al., 2017. Increased structural white and grey matter network connectivity compensates for functional decline in early multiple sclerosis. Mult Scler. 23 (3), 432–441.
Fleischer, V., Radetz, A., Ciolac, D., et al., 2019. Graph Theoretical Framework of Brain Networks in Multiple Sclerosis: A Review of Concepts. Neuroscience 1 (403), 35–53.
Giordano, A., Clarelli, F., Cannizzaro, M., et al., 2022. BDNF Val66Met polymorphism is associated with motor recovery after rehabilitation in progressive multiple sclerosis patients. Front. Neurol. 13, 790360.
Gonzalez-Escamilla, G., Muthuraman, M., Reich, M.M., et al., 2019. Cortical network fingerprints predict deep brain stimulation outcome in dystonia. Mov Disord. 34 (10), 1537–1546.
Gonzalez-Escamilla, G., Ciolac, D., De Santis, S., et al., 2020. Gray matter network reorganization in multiple sclerosis from 7-Tesla and 3-Tesla MRI data. Ann Clin Transl Neurol. 7 (4), 543–553.
Gonzalez-Escamilla, G., Koirala, N., Bange, M., et al., 2022. Deciphering the network effects of deep brain stimulation in parkinson's disease. Neurology and Therapy. 11 (1), 265–282.
Haider, L., Simeonidou, C., Steinberger, G., et al., 2014. Multiple sclerosis deep grey matter: the relation between demyelination, neurodegeneration, inflammation and iron. J Neurol Neurosurg Psychiatry. 85 (12), 1386–1395.
Herz, D.M., Little, S., Pedrosa, D.J., et al., 2018. Mechanisms underlying decision-making as revealed by deep-brain stimulation in patients with parkinson's disease. Curr Biol. 28 (8), 1169–78 e6.
Herz, D.M., Bange, M., Gonzalez-Escamilla, G., et al., 2022. Dynamic control of decision and movement speed in the human basal ganglia. Nat. Commun. 13 (1), 7530.
Holtzheimer, P.E., Kelley, M.E., Gross, R.E., et al., 2012. Subcallosal cingulate deep brain stimulation for treatment-resistant unipolar and bipolar depression. Arch. Gen. Psychiatry 69 (2), 150–158.
Huang, J., Khademi, M., Fugger, L., et al., 2020. Inflammation-related plasma and CSF biomarkers for multiple sclerosis. Proceedings of the National Academy of Sciences of the United States of America 117 (23), 12952–12960.
Isensee, F., Petersen, J., Kohl, S.A., Jäger, P.F., Maier-Hein, K.H., nnu-net,, 2019. Breaking the Spell on Successful Medical Image Segmentation. 1, 1–8 arXiv preprint arXiv:190408128.
Isensee, F., Jaeger, P.F., Kohl, S.A.A., Petersen, J., Maier-Hein, K.H., 2021. nnU-Net: a self-configuring method for deep learning-based biomedical image segmentation. Nat Methods. 18 (2), 203–211.
Jacobsen, C., Hagemeier, J., Myhr, K.M., et al., 2014. Brain atrophy and disability progression in multiple sclerosis patients: a 10-year follow-up study. J Neurol Neurosurg Psychiatry. 85 (10), 1109–1115.
Khawaldeh, S., Tinkhauser, G., Torrecillos, F., et al., 2022. Balance between competing spectral states in subthalamic nucleus is linked to motor impairment in Parkinson's disease. Brain 145 (1), 237–250.
Klistorner, S., Barnett, M.H., Parratt, J., Yiannikas, C., Graham, S.L., Klistorner, A., 2022. Choroid plexus volume in multiple sclerosis predicts expansion of chronic lesions and brain atrophy. Ann. Clin. Transl. Neurol. 9 (10), 1528–1537.
Kohler, C.A., Freitas, T.H., Maes, M., et al., 2017. Peripheral cytokine and chemokine alterations in depression: a meta-analysis of 82 studies. Acta Psychiatr Scand. 135 (5), 373–387.
Kramer, J., Meuth, S.G., Tenberge, J.G., Schiffler, P., Wiendl, H., Deppe, M., 2015. Early and degressive putamen atrophy in multiple sclerosis. Int. J. Mol. Sci. 16 (10), 23195–23209.
Kühner, C., Bürger, C., Keller, F., Hautzinger, M., 2007. [Reliability and validity of the Revised Beck Depression Inventory (BDI-II). Results from German samples]. Der Nervenarzt 78 (6), 651–656.
Little, S., Brown, P., 2012. What brain signals are suitable for feedback control of deep brain stimulation in Parkinson's disease? Ann N Y Acad Sci. 1265 (1), 9–24.
Little, S., Beudel, M., Zrinzo, L., et al., 2016. Bilateral adaptive deep brain stimulation is effective in Parkinson's disease. J Neurol Neurosurg Psychiatry. 87 (7), 717–721.
Lofredi, R., Tan, H., Neumann, W.J., et al., 2019. Beta bursts during continuous movements accompany the velocity decrement in Parkinson's disease patients. Neurobiol. Dis. 127, 462–471.
Maere, S., Heymans, K., Kuiper, M., 2005. BiNGO: a Cytoscape plugin to assess overrepresentation of gene ontology categories in biological networks. Bioinformatics 21 (16), 3448–3449.
Moraud, E.M., Tinkhauser, G., Agrawal, M., Brown, P., Bogacz, R., 2018. Predicting beta bursts from local field potentials to improve closed-loop DBS paradigms in Parkinson's patients. Annual International Conference of the IEEE Engineering in Medicine and Biology Society IEEE Engineering in Medicine and Biology Society Annual International Conference 2018, 3766–3796.
Müller, J., Noteboom, S., Granziera, C., Schoonheim, M.M., 2023. Understanding the role of the choroid plexus in multiple sclerosis as an MRI biomarker of disease activity. Neurology 100 (9), 405–406.
V.S. Natu J. Gomez M. Barnett et al. Apparent thinning of human visual cortex during childhood is associated with myelination Proceedings of the National Academy of Sciences of the United States of America 116 41 2019 20750 9.
Neumann, W.J., Memarian Sorkhabi, M., Benjaber, M., et al., 2021. The sensitivity of ECG contamination to surgical implantation site in brain computer interfaces. Brain Stimul. 14 (5), 1301–1306.
Ng PR, Bush A, Vissani M, McIntyre CC, Richardson RM. Biophysical Principles and Computational Modeling of Deep Brain Stimulation. Neuromodulation : journal of the International Neuromodulation Society. 2023 May 19.
Parodi, B., Kerlero de Rosbo, N., 2021. The gut-brain axis in multiple sclerosis. is its dysfunction a pathological trigger or a consequence of the disease? Frontiers in Immunology 12, 718220.
Polman, C.H., Reingold, S.C., Banwell, B., et al., 2011. Diagnostic criteria for multiple sclerosis: 2010 revisions to the McDonald criteria. Ann Neurol. 69 (2), 292–302.
Pravata, E., Rocca, M.A., Valsasina, P., et al., 2017. Gray matter trophism, cognitive impairment, and depression in patients with multiple sclerosis. Mult Scler. 23 (14), 1864–1874.
Ricigliano, V.A.G., Morena, E., Colombi, A., et al., 2021. Choroid Plexus Enlargement in Inflammatory Multiple Sclerosis: 3.0-T MRI and Translocator Protein PET Evaluation. Radiology 301 (1), 166–177.

Sacchet, M.D., Gotlib, I.H., 2017. Myelination of the brain in Major Depressive Disorder: An in vivo quantitative magnetic resonance imaging study. Sci. Rep. 7 (1), 2200.
Sacco, R., Santangelo, G., Stamenova, S., et al., 2016. Psychometric properties and validity of Beck Depression Inventory II in multiple sclerosis. Eur. J. Neurol. 23 (4), 744–750.
Schoonheim, M.M., Meijer, K.A., Geurts, J.J., 2015. Network collapse and cognitive impairment in multiple sclerosis. Front. Neurol. 6, 82.
Seemuller, F., Schennach, R., Musil, R., et al., 2023. A factor analytic comparison of three commonly used depression scales (HAMD, MADRS, BDI) in a large sample of depressed inpatients. BMC Psychiatry 23 (1), 548.
Sokolov, B.P., 2007. Oligodendroglial abnormalities in schizophrenia, mood disorders and substance abuse. Comorbidity, shared traits, or molecular phenocopies? The International Journal of Neuropsychopharmacology. 10 (4), 547–555.
Steenwijk, M.D., Geurts, J.J., Daams, M., et al., 2016. Cortical atrophy patterns in multiple sclerosis are non-random and clinically relevant. Brain 139 (Pt 1), 115–126.
Steffen, F., Uphaus, T., Ripfel, N., et al., 2023. Serum neurofilament identifies patients with multiple sclerosis with severe focal axonal damage in a 6-year longitudinal cohort. Neurology(R) Neuroimmunology & Neuroinflammation. 10 (1).
Szklarczyk, D., Gable, A.L., Nastou, K.C., et al., 2021. The STRING database in 2021: customizable protein-protein networks, and functional characterization of user-uploaded gene/measurement sets. Nucleic Acids Res. 49 (D1), D605–D612.
Tham, M.W., Woon, P.S., Sum, M.Y., Lee, T.S., Sim, K., 2011. White matter abnormalities in major depression: evidence from post-mortem, neuroimaging and genetic studies. J. Affect. Disord. 132 (1–2), 26–36.
Tinkhauser, G., Pogosyan, A., Little, S., et al., 2017. The modulatory effect of adaptive deep brain stimulation on beta bursts in Parkinson's disease. Brain 140 (4), 1053–1067.
Tinkhauser, G., Torrecillos, F., Duclos, Y., et al., 2018. Beta burst coupling across the motor circuit in Parkinson's disease. Neurobiol. Dis. 117, 217–225.
Vercellino, M., Votta, B., Condello, C., et al., 2008. Involvement of the choroid plexus in multiple sclerosis autoimmune inflammation: a neuropathological study. J Neuroimmunol. 199 (1–2), 133–141.
Vidal-Pineiro, D., Walhovd, K.B., Storsve, A.B., Grydeland, H., Rohani, D.A., Fjell, A.M., 2016. Accelerated longitudinal gray/white matter contrast decline in aging in lightly myelinated cortical regions. Hum Brain Mapp. 37 (10), 3669–3684.
Visser-Vandewalle, V., Andrade, P., Mosley, P.E., et al., 2022. Deep brain stimulation for obsessive-compulsive disorder: a crisis of access. Nat Med. 28 (8), 1529–1532.
Wang, Y.P., Gorenstein, C., 2013. Psychometric properties of the Beck Depression Inventory-II: a comprehensive review. Rev. Bras. Psiquiatr. 35 (4), 416–431.
Widge, A., Basu, I., Zorowitz, S., et al., 2019. Closed loop deep brain stimulation enhances cognitive control. Brain Stimulation: Basic, Translational, and Clinical Research in Neuromodulation 12 (2), 434.
Widge AS. Closing the loop in psychiatric deep brain stimulation: physiology, psychometrics, and plasticity. Neuropsychopharmacology : official publication of the American College of Neuropsychopharmacology. 2023 Jul 6.
Wittchen H-U, Zaudig M, Fydrich T. Skid. Strukturiertes klinisches Interview für DSM-IV. Achse I und II. Handanweisung. 1997.